2021 43rd Annual International Conference of the
IEEE Engineering in Medicine & Biology Society (EMBC)
Oct 31 - Nov 4, 2021. Virtual Conference

Wireless Electrocardiography and Impedance Cardiography Devices Using a Network Time Protocol for Synchronized Data

Stefano Orsolini[1], Enrico Pannicke[2,4], Ivan Fomin[3,4], Oliver Thieme[3,4], Georg Rose[3,4]

Abstract— **During minimally invasive and image-guided procedures, vital parameters have to be recorded for patient safety. In the Magnetic Resonance Tomograph (MRT) environment the Magneto Hydrodynamic (MHD) effect emerges, under the high magnetic field strength in the signal recording of an Electrocardiography (ECG) system. To allow the investigation of this effect, newly developed wireless ECG and Impedance cardiography (ICG) devices using a network time protocol for accurate synchronization of the collected data will be presented. The developed ICG and tetrapolar electrodes were designed to comply with the IEC 60601-1 standard. One subject was instructed to alternate phases of end-inspiration breath hold with the regular breathing cycle and concurrent synchronized ECG and ICG were collected.**

I. INTRODUCTION

ECG is a well accepted method for monitoring patient status in all kind of clinical settings and algorithms for cardiac abnormality diagnosis are being developed [1]. On the other hand ICG is a less common method for noninvasive monitoring but can be used to estimate stroke volume of the cardiac output [2]. Single devices for simultaneous measurement of ECG and ICG can be found on the market like the Task Force Monitor (CNSystems Medizintechnik GmbH, Graz, Austria) and also as subject of research [3], but with limitations in mobility, operability with other devices or data sampling frequencies. Moreover, purchased medical devices present the disadvantage that their internal structure is unknown and the processing algorithms are not publicly available. Therein lies the advantage of using self-built or open source devices in the context of research, to have full control over the hardware resources and data acquisition chains.

A field which would benefit from high sampling frequency ECG and simultaneous ICG is that of interventions which require the combined use of a MRT. In this context, the typical ECG cardiac complex appears combined with signals caused by the MHD effect [4]. As these signals correlate with blood flow, collecting the ICG would be beneficial in understanding how the MHD effect is influenced by the physiology of the subject. Use of a wireless ECG sampling at 1 kHz and a pressure sensing device for ballistocardiography inside a MRT was demonstrated by K.M. zu Hartlage et al.[5]. In that system the parts were synchronized by a TTL pulse to allow for multimodal analysis of the collected data but presenting limited ergonomics. This work presents two wireless devices, one for ECG and one for ICG, able to collect accurately synchronized data using a network time protocol, offering greater ergonomics and scalability than previous systems.

[1]Stefano Orsolini is with Department of Electrical, Electronic, and Information Engineering "Guglielmo Marconi", University of Bologna, Cesena, FC 47521, Italy stefano.orsolini@gmail.com

[2] Enrico Pannicke is with the Chair of Electromagnetic Compatibility, Otto-von-Guericke University, Magdeburg, SA 39106, Germany enrico.pannicke@ovgu.de

[3] Ivan Fomin, Oliver Thieme and Georg Rose are with the Chair in Healthcare Telematics and Medical Engineering, Otto-von-Guericke University, Magdeburg, SA 39106, Germany

[4] Enrico Pannicke, Ivan Fomin, Oliver Thieme and Georg Rose are involved with Research Campus *STIMULATE*, Otto-von-Guericke University, Magdeburg, SA 39106, Germany

II. METHODS

A. Architecture

All devices which are part of the network are based on the ESP32 (Espressif Systems, Shanghai), a micro-controller unit (MCU) with dual core central processing unit (CPU) which integrates simultaneous Bluetooth and Wi-Fi communications. Furthermore, a vast software library based on a real-time operating system (FreeRTOS) and a smartphone app which allows MCU connection to any custom access point (AP) are available online as open source (espressif.com).

To achieve accurate synchronization between timeseries for multimodal offline data analyses, a network time protocol is used instead of a physical trigger method to offer full functionality over different starting times of each device data acquisitions and ease of future expansion of the sensors' network, represented in Fig. 1. Simple network time protocol (SNTP) in particular presented the sufficient accuracy to synchronize data collected at 1000 samples per second (1 kSPS) reliably [6]. An AP established by a GNU Linux workstation runs the SNTP server for all connected devices to synchronize their respective global time variable then the collected data packets are timestamped at the time of creation by the MCU.

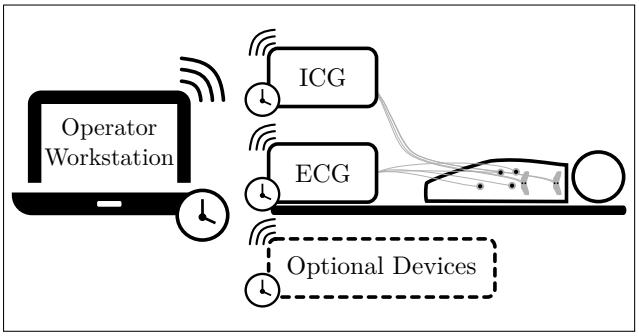

Fig. 1. Representation of the wireless network infrastructure. The Operator Workstation runs a SNTP server for all devices to synchronize to.

The workstation runs a Python software interface to configure acquisition parameters and collect data from a network protocol socket. User datagram protocol (UDP) was chosen for its ease of implementation and requiring fewer resources from the MCU than transmission control protocol (TCP) [7].

A single packet includes data from a fixed number of sampling cycles (N_{cycles}) therefore the time between packets is a value that can be computed from the sampling frequency F_s. Packet loss detection is implemented as a timeout of value N_{cycles}/F_s on the receiving UDP socket to trigger an error message to the software interface during data acquisition. Moreover, during offline analysis, signal integrity can be verified checking the contiguity of the SNTP timestamps associated to the received packets. N_{cycles} can be set arbitrarily to trade-off between MCU resources and streaming performance. UDP throughput is in the order of $10\,\text{Mb/s}$ [8] therefore the set of connected devices must be verified to operate below this limit. Data rate is calculated and presented for each device by the software interface.

To allow for a clear interaction of the operator with the developed devices, an integrated capacitive sensor on the ESP32 MCU is used as a touch button for controlling power up and down, together with an LED to signal when the device is operative or turned off (Fig. 2).

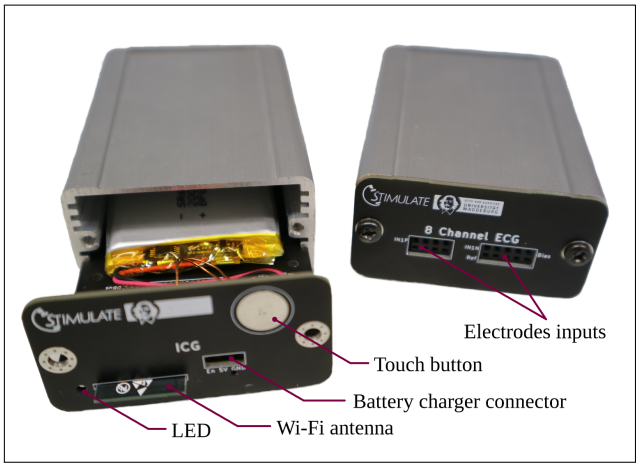

Fig. 2. ICG (front side) and ECG (back side) devices supplied by a Li-ion battery within $80 \times 59 \times 30\,\text{mm}$ aluminium enclosures.

B. ECG

To collect the ECG signal, the Texas Instruments ADS1299 SPI peripheral is used. This component integrates 8 low-noise differential channels with 24-bit ADCs and an analog front end with programmable gain amplifiers (PGA) and $1\,\text{G}\Omega$ input impedance making it a reference integrated circuit for acquisition of biopotentials in battery powered systems.

The ADS1299 allow to configure the F_s from $250\,\text{SPS}$ up to $16\,\text{kSPS}$, in the presented device $1\,\text{kSPS}$ resulted as the highest F_s achievable at the lowest CPU frequency setting of $80\,\text{MHz}$. $2\,\text{kSPS}$ could be achieved with the CPU at $240\,\text{MHz}$ but at the cost of increased energy requirements. For the ECG device, N_{cycles} is set at 125 giving a packet size of $3.137\,\text{kBytes}$ for a resulting data rate of $25.096\,\text{kBytes/s}$.

Commercially available MR compatible adhesive electrodes with solid gel are used for acquisition of the ECG signals. The common ground is applied to the right leg while reference electrode in correspondence of the heart apical pulse and the 8 channels distributed uniformly on the chest.

ECG signal is converted from raw data to volts taking into account the ADC specifications and PGA setting.

C. ICG

To collect the ICG signal the Analog Devices AD5933 I^2C peripheral is used. This component integrates a frequency generator from $1\,\text{kHz}$ to $100\,\text{kHz}$ and a 12-bit ADC with on-board digital signal processor (DSP) for discrete Fourier transformation (DFT) calculation of the response signal. The presented design is largely based on the original concept by Noveletto et al. (2016) where the AD5933 is used together with a modified mirrored Howland current source and an instrumentation amplifier as an analog front end to acquire the ICG signal from a tetrapolar electrodes' configuration [9].

To reduce the load common mode voltage and enhance the load capability of the current source, the modified mirrored Howland current source by Noveletto is replaced by an implementation of the Quad-feedback enhanced Howland current source (QUAD-EHCS) conceptually introduced by Sirtoli et al. (2018) [10]. An LTspice simulation of the QUAD-EHCS using an Analog Devices AD8132 differential amplifier was used to adjust components values before manufacturing. The circuit was designed to have a $1\,\text{kHz}$ to $100\,\text{kHz}$ passband and to generate a current within the limits of the IEC 60601-1 guidelines regarding DC and AC current delivered to the body [11]. A sinusoidal current at $70\,\text{kHz}$ is employed and the current source calibrated on a purely resistive load to deliver $700\,\mu\text{A}_{\text{rms}}$ when the AD5933 is set to maximum excitation voltage ($1.98\,\text{V}_{\text{p-p}}$).

As instrumentation amplifier to collect the voltage difference on the subject body, a Texas Instruments INA118 is used, acting as band-pass filter in the $1\,\text{kHz}$ to $100\,\text{kHz}$ range limiting the received signal to the bandwidth of the sinusoidal generator.

The data collection rate for the DFT is limited by three main factors: the conversion process takes approximately $1\,\text{ms}$, the I^2C bus clock frequency is limited (max. $400\,\text{kHz}$), the peripheral registers need to be reprogrammed to run a new measurement even when the stimulation frequency is unchanged. $500\,\text{SPS}$ appeared as an upper limit to the achievable data rate from the peripheral but $250\,\text{SPS}$ is used given the low frequency content of the ICG signal (much inferior to $100\,\text{Hz}$). For the ICG device, N_{cycles} is set at 125 giving a packet size of $635\,\text{Bytes}$ for a resulting data rate of $1.27\,\text{kBytes/s}$.

ICG signal is computed from the magnitude of the DFT results to which smoothing is applied with a centered moving average filter (window length $0.1\,\text{s}$). First time derivative is then computed and sign is inverted. The resulting value gives

an uncalibrated estimate of combined blood flow velocity and blood volume change [2].

Two set of electrodes have been tested for measurement of the ICG signal, one disposable type commercially available for the Task Force Monitor and a reusable custom set developed with flexible electronics manufacturing techniques. Both electrode designs are specifically intended for a neck-abdomen electrode application, a configuration typically used for thoracic bioimpedance measurements. The design of the custom electrode presents a larger surface for current injection (I_{gen}) and a smaller one for voltage measurement (V_{ina}). Shown in Fig. 3 are the manufactured custom electrode pair with non magnetic steel button terminals and coating by immersion tin [Sn] process for biocompatibility of the conductive surfaces. The custom electrodes are applied to the skin using a conductive gel and are fixed in place with medical grade adhesive tape.

Fig. 3. Custom manufactured flexible electrode pair for ICG with tin [Sn] coating on the front and nonmagnetic steel button terminals on the back.

To interpret the electrical measurements of the electrodes, a simplified model of the impedance network seen by the analog front end was used (Fig. 4). The load under test is composed by the series of steady valued Z_{body} due to conduction and dispersion mechanisms in the body [12] and the variable impedances Z_{breath} and Z_{cardio} which respectively encompass modulation phenomena due to breathing and cardiac activity. Additionally the 4 electrode-to-skin impedances ($R_{\text{gen}}||C_{\text{gen}}$ and $R_{\text{ina}}||C_{\text{ina}}$) are considered.

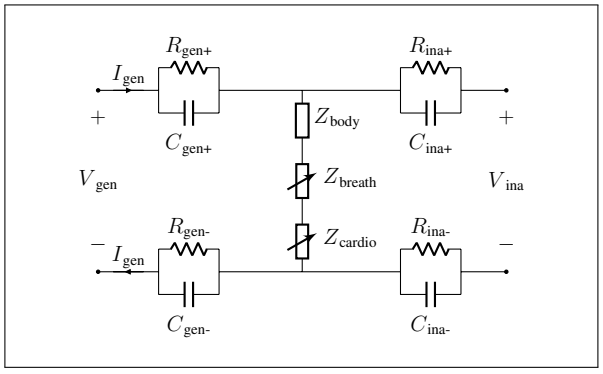

Fig. 4. Simplified model of human body load for impedance measurement.

D. Experimental protocol

Subject was instructed to alternate phases of end-inspiration breath hold with the regular breathing cycle. Breath hold for the ICG signal is the electrical analogous of reducing the variable Z_{breath} to a steady-valued impedance for the model in Fig. 4.

DC and AC_{rms} values of the delivered current I_{gen} were measured from electrodes applied on a subject using a true-RMS multimeter placed in series to one of the current generator lines. Voltage nodes were measured using a 4 channel oscilloscope with inputs referred to the developed device common ground. Then the oscilloscope data from a time span encompassing 3 cycles of the delivered sinusoidal signal were exported for analysis. Difference signals were calculated (i.e. $V_{\text{gen}} = V_{\text{gen}}{}^{+} - V_{\text{gen}}{}^{-}$; $V_{\text{ina}} = V_{\text{ina}}{}^{+} - V_{\text{ina}}{}^{-}$), arithmetic average values (DC) and root mean square of the demeaned values (AC_{rms}) were extracted and loads estimated as $Z_{\text{gen}} = V_{\text{gen}}/I_{\text{gen}}$ and $Z_{\text{ina}} = V_{\text{ina}}/I_{\text{ina}}$.

The tetrapolar configuration for impedance measurement has the property of measuring the voltage drop across the load under test (estimated as Z_{ina}) regardless of electrode-to-skin impedances because negligible current is flowing towards or from the instrumentation amplifier whereas estimation of Z_{gen} comprises electrode-to-skin impedances.

III. RESULTS

A. ICG electrode

Measurement results are reported in Tab. I and Tab. II. The Z_{gen} values result larger than Z_{ina}, both for the DC and AC_{rms} components, in agreement with expectations from a tetrapolar impedance measurement. For both electrodes specification limit for the delivered current to the body (I_{gen}) is respected.

TABLE I

ELECTRICAL RESULTS WITH CUSTOM DEVELOPED ICG ELECTRODE

	$I_{\text{gen}}[\mu\text{A}]$	$V_{\text{gen}}[\text{mV}]$	$Z_{\text{gen}}[\Omega]$	$V_{\text{ina}}[\text{mV}]$	$Z_{\text{ina}}[\Omega]$
DC	6	-18	3k	9	1.5k
AC_{rms}	649	68	105	37	57

TABLE II

ELECTRICAL RESULTS WITH TASK FORCE MONITOR ICG ELECTRODE

	$I_{\text{gen}}[\mu\text{A}]$	$V_{\text{gen}}[\text{mV}]$	$Z_{\text{gen}}[\Omega]$	$V_{\text{ina}}[\text{mV}]$	$Z_{\text{ina}}[\Omega]$
DC	7	-86	12k	30	4k
AC_{rms}	645	97	151	38	59

B. Concurrent ECG and ICG measurements

Presented in Fig. 5 are 4 s ECG and ICG signals collected from the subject during end-inspiration breath hold. ECG signal corresponding to the conventional *Lead II* derivation. Signals acquired during regular breathing are presented in Fig. 6 for a time span of 20 s to encompass multiple breathing cycles.

IV. CONCLUSIONS

A wireless 8 channel ECG sampling at 1 kSPS and a wireless tetrapolar ICG sampling at 250 SPS were built.

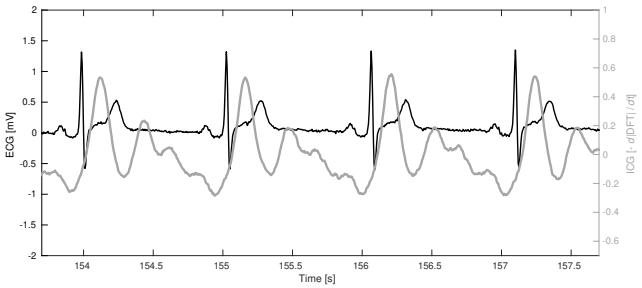

Fig. 5. Measuring 4 s of end-inspiration breath hold concurrent ECG Voltage (left axis) and ICG (right axis) signals.

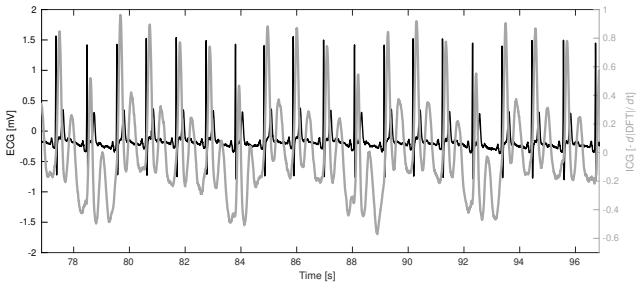

Fig. 6. Measurement during regular breathing (20 s) concurrent ECG (left axis) and ICG (right axis) signals.

Accurate time series alignment for multimodal data analysis is achieved by synchronizing the devices to a SNTP server and timestamp the data at the time of collection. The ICG was designed and tested to meet the safety standards for medical electrical equipment [3]. The overall performance of each single device is limited by the resources of the chosen MCU (i.e. bus clock, CPU frequency). The results of the ICG signal is showing a voltage offset shift according to the respiration cycle of the subject, see Fig. 6, therefore in the experimental protocol the subject had been instructed to hold breath for a few seconds to allow an ICG measurement unbiased from the breathing component, see Fig. 5.

If needed, the system architecture can be scaled with the inclusion of more custom-built wireless devices (e.g. pulse oximeters, pressure meters). Its affordability would make it a feasible technological platform for establishing multicentric studies, data collected from subject groups would conform to the same standards of quality and security and be made easily available to the scientific community. In future work, the system will be made compliant for use in an MRT where time synchronous data sampling of ECG and ICG would significantly enhance the study of the MHD effect generated by vessel blood flow.

APPENDIX

Link to the repository overview of the project EMERGE https://github.com/OliverThieme/Emerge.git

ACKNOWLEDGMENT

The work of this paper is partly funded by the EFRE project Saxony-Anhalt WISSENSCHAFT under the grant number ZS/2016/04/78123, the Federal Ministry of Education and Research within the Research Campus *STIMULATE* under the number '13GW0473A' and the project EMERGE under the number '13GW0415B'.

All procedures performed in studies involving human participants were in accordance with the ethical standards of the institutional and/or national research committee and with the 1964 Helsinki Declaration and its later amendments or comparable ethical standards. Informed consent was obtained from all individual participants involved in the study.

REFERENCES

[1] D. Borra, A. Andaló, S. Severi, and C. Corsi, "On the Application of Convolutional Neural Networks for 12-lead ECG Multi-label Classification Using Datasets From Multiple Centers," in 2020 Computing in Cardiology, Sep. 2020, pp. 1–4, doi: 10.22489/CinC.2020.349.

[2] D. P. Bernstein, "Impedance cardiography: Pulsatile blood flow and the biophysical and electrodynamic basis for the stroke volume equations," Journal of Electrical Bioimpedance, vol. 1, no. 1, pp. 2–17, Dec. 2009, doi: 10.5617/jeb.51.

[3] Abdelakram Hafid, Sara Benouar, Malika Kedir-Talha, Mokhtar Attari, Fernando Seoane, "Simultaneous Recording of ICG and ECG Using Z-RPI Device with Minimum Number of Electrodes", Journal of Sensors, vol. 2018, Article ID 3269534, 7 pages, 2018. https://doi.org/10.1155/2018/3269534

[4] J. W. Krug and G. Rose, "Magnetohydrodynamic distortions of the ECG in different MR scanner configurations," in 2011 Computing in Cardiology, Sep. 2011, pp. 769–772.

[5] K. M. zu Hartlage, E. Pannicke, S. Orsolini, G. Rose, R. Vick, and J. K. Passand, "Patient Monitoring During Magnetic Resonance Imaging Exams by Means of Ballistocardiography," in 2019 Computing in Cardiology (CinC), Sep. 2019, p. Page 1-Page 4, doi: 10.23919/CinC49843.2019.9005783.

[6] M. Ussoli and G. Prytz, "SNTP time synchronization accuracy measurements," in 2013 IEEE 18th Conference on Emerging Technologies Factory Automation (ETFA), Sep. 2013, pp. 1–4, doi: 10.1109/ETFA.2013.6648120.

[7] E. Gamess and B. Smith, "Performance Evaluation of TCP and UDP over IPv4 and IPv6 for the ESP8266 Module," in Proceedings of the 2020 2nd International Electronics Communication Conference, New York, NY, USA, Jul. 2020, pp. 161–169, doi: 10.1145/3409934.3409956.

[8] A. L. Wijesinha, Yeong-tae Song, M. Krishnan, V. Mathur, J. Ahn, and V. Shyamasundar, "Throughput measurement for UDP traffic in an IEEE 802.11g WLAN," in Sixth International Conference on Software Engineering, Artificial Intelligence, Networking and Parallel/Distributed Computing and First ACIS International Workshop on Self-Assembling Wireless Network, May 2005, pp. 220–225, doi: 10.1109/SNPD-SAWN.2005.76.

[9] F. Noveletto, P. Bertemes-Filho, and D. Dutra, "Analog Front-End for the Integrated Circuit AD5933 Used in Electrical Bioimpedance Measurements," in II Latin American Conference on Bioimpedance, Singapore, 2016, pp. 48–51, doi: 10.1007/978-981-287-928-8_13.

[10] V. G. Sirtoli, K. F. Morcelles, and V. C. Vincence, "Design of current sources for load common mode optimization," Journal of Electrical Bioimpedance, vol. 9, no. 1, pp. 59–71, Dec. 2018, doi: 10.2478/joeb-2018-0011.

[11] IEC 60601-1:2005, Leakage Currents and Patient Auxiliary Currents (8.7.3 b)

[12] S. Grimnes and O. G. Martinsen, "Cole electrical impedance Model-a critique and an alternative," IEEE Transactions on Biomedical Engineering, vol. 52, no. 1, pp. 132–135, Jan. 2005, doi: 10.1109/TBME.2004.836499. 30 Apr. 2012, doi:10.3402/jchimp.v2i1.14383